CHAPTER 163

# SIMULATION OF WAVE FORCES ON A HORIZONTAL CYLINDER

SUSUMU TSUZUKI*
KIYOSHI HORIKAWA** F.ASCE
AKIRA WATANABE***

ABSTRACT

The characteristics of wave forces acting on a horizontal circular cylinder were investigated through numerical calculations as well as experimental findings. The laboratory data on wave forces were analyzed by the concept of wave force path and classified into two types. One is the circular type and the other one is the 8 - shaped type. In order to analyze the above phenomena, the discrete vortex method was applied with appropriate assumptions. The comparison between the numerically calculated results and laboratory data shows that the simulation model proposed in this paper seems to be favorable to predict the wave forces acting on a horizontal circular cylinder within a certain range of conditions.

## 1. INTRODUCTION

Prediction of wave forces acting on a circular cylinder has been investigated by number of researchers during the last thirty eight years since Morison et al. (1950) proposed their semi-empirical formula. The main interest of these researchers was to evaluate the hydrodynamic coefficients introduced in the stated formula (Koderayama et al., 1978). However, the formula cannot be applied to such a case that vorticies generated behind a circular cylinder are extremely unsymmetrical with respect to wave direction.

In the present paper, an analytical and numerical treatment was attempted to calculate the flow characteristics around a horizontal circular cylinder induced by gravity waves or oscillatory flows and the fluid forces acting on the body by using the discrete vortex

* Engineer, Tokyo Electric Co.
** Professor Emeritus, The University of Tokyo ; Professor, Saitama University, Urawa, Japan.
*** Professor, Department of Civil Engineering, The University of Tokyo, Japan.

method which was originally presented by Rosenhead (1931). The above treatment was carried out under such a restricted condition that the effects of free surface as well as of the bottom on fluid motion can be neglected. That is to say, it is assumed that the submerged cylinder is located in a certain range of water depth apart from the limited layers of both free surface and sea bed. The calculated results were compared with the experimental data reported by Sarpkaya (1975) in order to investigate the adaptability of the stated prediction method.

## 2. CHARACTERISTICS OF WAVE FORCES ACTING ON A HORIZONTAL CIRCULAR CYLINDER

### 2.1 Previous Studies

It is well known that the Morison formula is commonly applied to evaluate the wave forces acting on a cylinder, particularly on a circular cylinder. However, in the case of a submerged circular cylinder set horizontally at a certain water depth, the direction of wave force acting on the cylinder varies with time, the situation of which is different from that of a vertical cylinder. Hence the Morison formula was extended by Borgman (1958) to the vectorial form, under the assumption that the direction of drag force is the same to that of fluid velocity.

However the above assumption is not necessary to be true. Therefore Sawamoto et al. (1979) investigated the fluid force induced by oscillatory flows, and Tsuzuki et al. (1984) and Masuda et al. (1985) did by wave by introducing a phase difference. According to the result of flow visualization conducted at the University of Tokyo, it is realized that the Morison type formula can not be applied to the case in which the motion of vortices separated from the body surface is complicative.

As a theoretical approach, Sarpkaya (1968) applied the Blasius formula for unsteady flow to calculate the fluid force on a circular cylinder under uniformly oscillating flows. Detailed observations made by Sawamoto and Kikuchi (1979) in an oscillatory flume indicated that the pattern of vortex formation can be classified by using the Keulegan-Carpenter number as shown in Figure 1. The Keulegan-Carpenter number is defined by $K.C.=\hat{U}T/2R$, where $\hat{U}$ is the amplitude of oscillatory flow velocity, $T$ the period of oscillatory flow, and $R$ the radius of the circular cylinder. From this diagram we can realize that the unsymmetrical vortices appear under the condition of $K.C. > 8$, causing nearly regular time variation of lift force.

### 2.2 Experimental Findings

In order to look at the above phenomena in an oscillatory flume more clearly, let us take the wave force path defined by the diagram illustrated in Figure 2. Here two kinds of typical laboratory data were picked up and drawn in Figure 3 for demonstration. The upper diagram indicates that the wave fore path for $K.C. = 4.24$ forms a

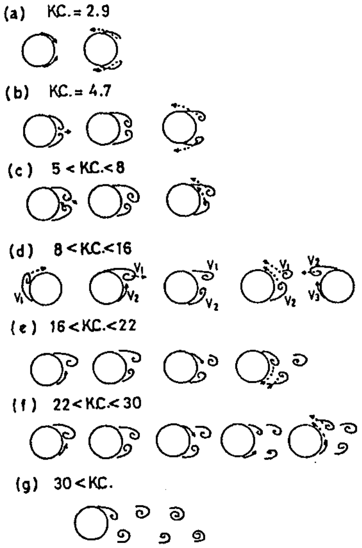


Fig.1 Vortex formation in an oscillatory flow ( after Sawamoto and Kikuchi, 1979 ).

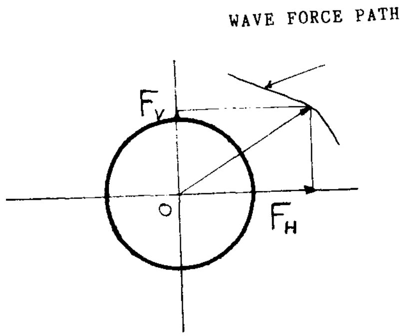


Fig.2 Definition of wave force path.

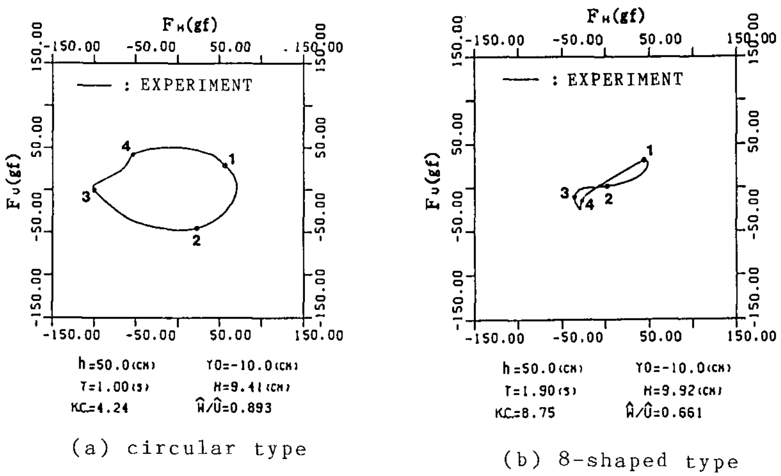


Fig.3 Typical examples of wave force path.

nearly circular curve, while the lower diagram indicates that the path for K.C. = 8.75 forms an 8 - shaped curve.

The situation of vortex formation in a wave field might be somewhat different from that in a uniformly oscillating flow. The laboratory data collected in a wave flume at the University of Tokyo were plotted as shown in Figure 4. The abscissa of this diagram is the K.C. number and the ordinate is the amplitude ratio between the vertical and horizontal fluid particle velocity amplitudes, $\hat{V}$ and $\hat{U}$. The open marks are for the circular type wave force path, which is called C type, and the filled marks for the wave force path with the 8 - shaped curve, which is E type. The upper part of the ordinate in this diagram corresponds to the deeper water wave condition, while the lower part corresponds to the shallower water wave condition. A demarcation curve between these two types of wave force path can not be clearly drawn. However, it can be said that E type appears under the shallower water and larger K.C. number conditions.

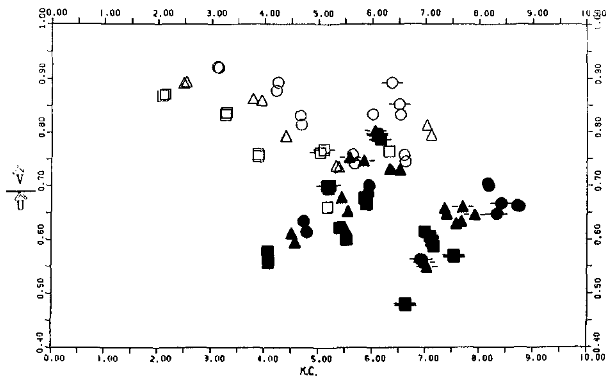


| C | E | $y_0$ (cm) | h (cm) |
|---|---|---|---|
| ○ | ● | -10 | 60.0 |
| △ | ▲ | -13 | |
| □ | ■ | -16 | |
| -○- | -●- | -10 | 50.0 |
| -△- | -▲- | -15 | |
| -□- | -■- | -20 | |

Fig.4

Wave force path data obtained in a wave flume.

## 3. SIMUMATION OF WAVE FORCES ACTING ON A HORIZONTAL CIRCULAR CYLINDER

### 3.1 Treatment for Simulation

#### (1) Discrete vortex method

The aim of this paper is to analyze the stated phenomena under appropriate conditions and assumptions. In the present treatment the discrete vortex method is applied. The following analysis is based on the potential flow theory in which the discrete vortices emitted from the horizontal circular cylinder surface are introduced. At first the Milne-Thomson circular theorem (Milne-Thomson, 1968) is used to determine the complex potential of the interested flow, however the free surface and bottom boundary make the analytical treatment extremely complex. According to Ogilvie (1963) and Chaplin (1981) it is concluded that the free surface effect on the boundary condition can be neglected when the ratio between the submerged water depth and the circular cylinder diameter is large enough, say 5. While Nath and Yamamoto (1974), and Uekita and Yamazaki (1980) investigated the effect of bottom boundary on the complex potential of the stated phenomena, and concluded that the bottom boundary effect can be neglected when the clearance between the lower portion of the cylinder and the bottom is larger than the circular cylinder diameter. Taking into account the above two results we will select an appropriate range of submergence of the circular cylinder in order to proceed the analysis in neglecting the surface and bottom boundary effects.

Now let us assume that the questioned complex potential, W, is the summation of those of potential flow surrounding a circular cylinder and of distrete vortices, $W_p$ and $W_v$. That is to say,

$$W = W_p + W_v \tag{1}$$

#### (2) Determination of $W_p$

The term Wp can be expressed in the next equation by using the Milne-Thomson circular theorem,

$$W_p = W_{p0}(z) + \overline{W_{p0}(R^2/\bar{z})} \tag{2}$$

where $W_{po}(z)$ is the complex potential for the flow field where the circular cylinder does not exist, and z=x+iy. In order to express the term explicitely, we are able to apply an appropriate wave theory such as the small amplitude wave theory, the finite amplitude wave theory, and the stream function theory. In case of the small amplitude wave theory

$$W_{p0} = \frac{\omega H}{2k \sinh kh} \sin(kz + iks_0 - \omega t) \tag{3}$$

where $\omega$ is the angular frequency, k the wave number, H the wave height, h the water depth, $s_0$ the distance of the circular cylinder center from the bed, and t the time. While in case of the stream function theory (Dean, 1965)

$$W_{p0} = -A_0 z + \sum_n A_n \sin(k_n z + i k_n s_0 - \omega_n t - \beta_n) \tag{4}$$

where $A_n$, $\beta_n$ are coefficient and phase lag appeared in the stream function theory, $k_n$ = nk, and $\delta_n = n\delta$.

(3) Determination of $W_v$

The term $W_v$ induced by discrete vortices can be expressed in the next equation by using again the Milne-Thomson circular theorem,

$$W_v = -\frac{i}{2\pi}\sum_k \Gamma_k \log(z - z_k) + \frac{i}{2\pi}\sum_k \Gamma_k \log(z - R^2/\bar{z}_k) \tag{5}$$

where $\Gamma_k$ and $z_k$ are the circulation and the complex position of each discrete vortex.

(4) Emission of a vortex and the vortex motion

In order to clarify the emission of a vortex from the circular cylinder surface, the location and the circulation of a vortex just before separating from the circular cylinder must be evaluated. From such a view point, the separation point is neccesary to be determined by any appropriate way. As a first step, we calculated the velocity distribution within a laminar boundary layer developed along the surface of a circular cylinder. However, it is quite natural that the above treatment can not be applied to the case with large K.C. numbers and large Reynods numbers. In order to determine the separation point in the above case, we decided to adopt the fllowing two conditions. The first one is that the shear stress on the cylinder surface, $\tau_b$, is zero at the separation point, the condition of which is commonly applied to the steady boundary layer flow. The second one is that the arcwide pressure gradient on the surface is zero at the separation point. The latter condition is adopted by the following reasons ; that is, (1) the flow separation may appear in the vicinity of the point on the surface where the pressure reaches its maximum, and (2) the stated position can be easily determined by using the potential flow velocity outside the boundary layer.

In order to check which condition is more suitable for our purpose, we applied the above two to the uniformly oscillating flow and compared the evaluted time dependent separation point with the laboratory data obtained by Grass and Kemp (1979) as shown in Figure 5. The abscissa indicates the phase of flow and the ordinate indicates the location of flow separation point on the cylinder surface. Either of these two conditions is not adequate to predict precisely the location of flow separation, however the condition for pressure gradient is better than that for shear stress. Therefore we selected the condition of pressure gradient to determine the flow separation point in

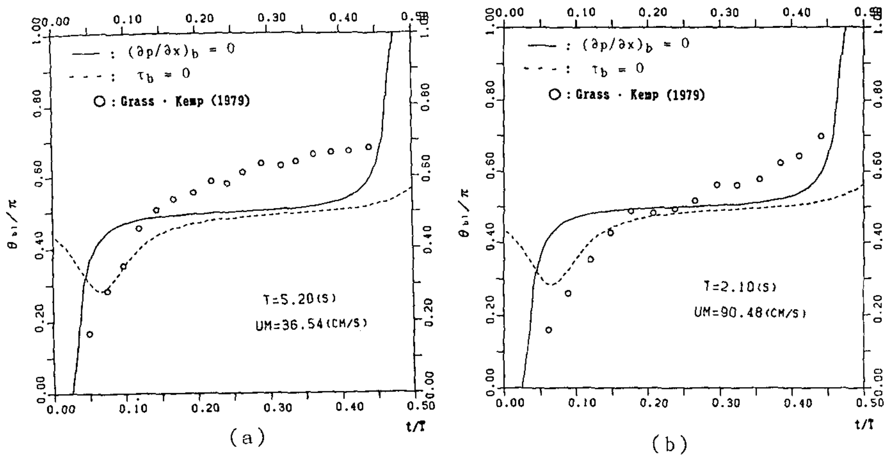


Fig.5 Comparison between predicted separation points and laboratory data

wave fields too.

The vortex flux, $\partial\Gamma/\partial t$, accumulated within the boundary layer in a unit time can be expressed by

$$\frac{\partial\Gamma}{\partial t} = \int_0^{\delta}\left(\frac{\partial v}{\partial x} - \frac{\partial u}{\partial y}\right)u\,dy \tag{6}$$

where $\delta$ is the thickness of boundary layer. Considering that the term $\partial v/\partial x$ is negligible comparing with the term $\partial u/\partial y$, we applied the following equation which was proposed by Sarpkaya (1968) as an approximate expression,

$$\frac{\partial\Gamma}{\partial t} = \frac{1}{2}U_B|U_B| \tag{7}$$

where $U_B$ is the velocity just outside the boundary layer at the separation point.

Next we assumed that the discrete vortex separated from the cylinder surface is moving with the velocity $(u_k, v_k)$, which can be calculated by the following equation

$$u_k - iv_k = \frac{d}{dz}\left\{W + \frac{i\Gamma_k}{2\pi}\log\,(z - z_k)\right\} \tag{8}$$

Therefore the position of the questioned vortex at the time step, $t + \Delta t$, can be determined as

$$z_k(t+\Delta t) = z_k(t) + (u_k, v_k)\Delta t \tag{9}$$

(5) Wave forces acting on a circular cylinder

The wave force components can be obtained by the Blasius formula for an unsteady flow by using the complex velocity potential. That is

$$F_H - iF_V = \frac{i\rho}{2}\oint_C \left(\frac{dW}{dz}\right)^2 dz + i\rho\frac{\partial}{\partial t}\oint_C \overline{W} d\bar{z} \tag{10}$$

where C is an arbitrary closed curve surrounding the questioned cylinder section. Introducing Equations (1), (2) and (5) into Equation (10), we get the next equation,

$$\begin{aligned} F_H - iF_V = {} & 2\pi\rho R^2 \frac{\partial}{\partial t}\left(\frac{\partial W_{p0}}{\partial z}\right) + 2\pi\rho R^2 \frac{\overline{\partial W_{p0}}}{\partial z}\frac{\partial W_{p0}}{\partial z} \\ & - i\rho \sum_k \Gamma_k (u_k - iv_k) - \rho \sum_k \overline{i\frac{\partial}{\partial t}(\Gamma_k R^2/\bar{z}_k)} \\ & + i\rho \sum_k \Gamma_k \frac{\partial^2 W_{p0}}{\partial z^2}(z_k - R^2/\bar{z}_k) \end{aligned} \tag{11}$$

(6) Decay of vortex circulation

In the treatment of the discrete vortex method, it is assumed that the circulation of emitted vortex maintains its original value. However the above assumption can not treate the actual phenomena due to the decay of vortices by the fluid viscosity. Considering the above fact, we will introduce the decay of vortex in the following way to simulate the flow characteristecs surrounding the horizontal circular cylinder. That is to say, we assume that the discrete vortex is represented by a Rankine vortex with a core, the radius of which, $r_v$, can be expressed by

$$r_v = 2.24\sqrt{\nu t^*} \tag{12}$$

where $t^*$ is the elapsed time since the vortex emitted from the cylinder surface and $\nu$ is the kinematic viscosity of fluid. The term $r_v$ corresponds to the core radius of Stokes vortex. In addition to the above, we also assume that the elapsed time, $t^*$, has its upper value $T_c$, which represents a kind of decay time. Hence the limited core radius, $r_c$, is given by

$$r_{cr} = 2.24\sqrt{\nu T_c} \tag{13}$$

(7) Calculation procedures

The flow chart of the numerical calculation is shown in Figure 6. That is to say, emit a discrete vortex at each time step, then calculate the velocity field, wave force acting on a cylinder and the translation of the above vortex. Repeat the above calculation proceses until the time history of wave forces reaches its cyclic pattern. When two discrete vortices come in touch each other, let unite them to a single vortex in such a way to conserve the total angular momentum. When the vortex comes inside of the circular cylinder, return the vortex to the position where the vortex core comes in touch with the cylinder surface, and then let the vortex be convected by the induced flow velocity at the next time step.

3.2 Numerical Results and Verification

(1) Conditions of numerical calculations

Numerical calculations were made for the flow characterestics near the horizontally immersed circular cylinder 1) under a uniformly oscillating flow and 2) under progressive waves. Tables 1 and 2 give the various conditions of calculations for a uniformly oscillating flow and for progressive waves respectively.

Throughout the numerical calculations, the time histories of total wave force, fluid force induced by vortices, and circulation of emitted vortices were printed out in graphical forms for three to four wave cycles. In addition to these, streamlines at various time steps were illustrated to look at visually the behavior of vortices emitted from the cylinder surface.

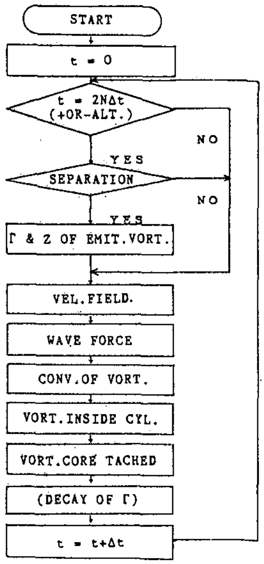


Fig.6

Flow chart

(2) Wave forces

In case of uniformly oscillating flow, it is clearly observed from the calculated results that the vortex motion becomes unsymmetrical and induces the lift force, the magnitude of which is comparable to the drag force in the direction of flow with the increase of K.C. number.

While in the case of progressive waves, the following conclusions were obtained :

1) The lift force has the magnitude comparable to the drag force and is mainly induced by the vortex motion.
2) In general the time histories of wave forces are apt to be cyclic by the introduction of vortex decay.
3) Under the deep water wave condition, the wave force has a single modal peak. But under the intermediate water wave condition, the drag force has a single peak over one wave cycle, while the lift force has bimodal peaks due to the unsymmetrical behavior of emitted vortices.
4) In Case W-1, the flow pattern and calculated wave forces were not influenced by the strength of vortex decay. However in Cases W-2 and W-3, these strongly depend on the strength of vortex decay.

(3) Wave force path

In order to investigate the effect of vortex decay, the calculated wave force pathes based on the stream function theory were compared with the laboratory data of Masuda et al. (1985) as shown in Figure 7. The solid lines are the experimental results, while the dotted lines are the calculated ones. The calculated curves in the upper

Table 1 Conditions for a uniformly oscillating flow.

(a) Calculation conditions

| Case | R (cm) | 1 (cm) | T (s) | U cm/s | K.C. | T/Δt |
|---|---|---|---|---|---|---|
| S-1 | 2.5 | 20.0 | 1.0 | 20.5 | 4.1 | 60 |
| S-2 | 2.5 | 20.0 | 1.4 | 22.9 | 6.4 | 80 |
| S-3 | 2.5 | 20.0 | 1.9 | 21.8 | 8.3 | 120 |

R : circular cylinder diameter, 1 : cylinder length, T : oscillatory flow period, U : horizontal velocity amplitude, K.C. : Keulegan-Carpenter number, $\Delta t$ : time step.

(b) Calculation runs for each case

| Run | Flow pattern | Decay of vortex |
|---|---|---|
| 1 | a) Symmetrical | Without |
| 2 | | With ( Tc = T ) |
| 3 | | With ( Tc = T/2 ) |
| 4 | b) Unsymmetrical | With ( Tc = T ) |
| 5 | | With ( Tc = T/2 ) |

Table 2 Conditions for progressive waves.

(a) Calculation conditions

| Case | R (cm) | 1 (cm) | h (cm) | Yo (cm) | T (s) | H (cm) | T/Δt |
|---|---|---|---|---|---|---|---|
| W-1 | 2.5 | 20.0 | 50.0 | 10.0 | 1.0 | 9.4 | 60 |
| W-2 | 2.5 | 20.0 | 50.0 | 13.0 | 1.4 | 11.0 | 80 |
| W-3 | 2.5 | 20.0 | 50.0 | 10.0 | 1.9 | 9.9 | 120 |

h : water depth, Yo : cylinder center depth,
H : wave height, others : same as in Table 1.

(b) Calculation runs for each case

| Run | Decay of vortex |
|---|---|
| 1 | Without |
| 2 | With ( Tc = T ) |
| 3 | With ( Tc = T/2 ) |

Note : Small amplitude wave theory and stream function theory were applied for calculations.

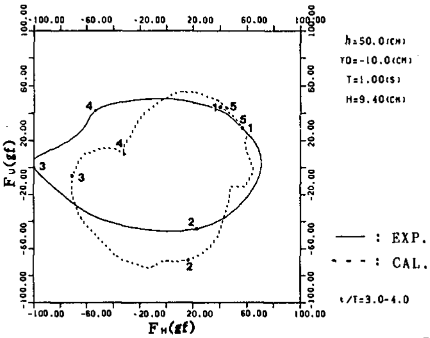


Tc = T

Fig.7 (a)

Comparison between calculated wave force path and laboratory data ( C-type ).

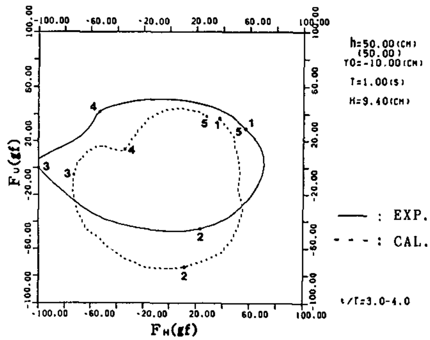


Tc = T/2

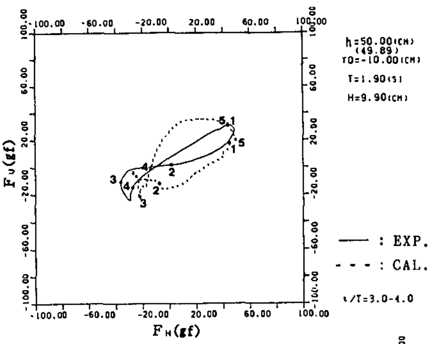


Tc = T/2

Fig.7 (b)

Comparison between calculated wave force path and laboratory data ( E-type ).

Tc = T

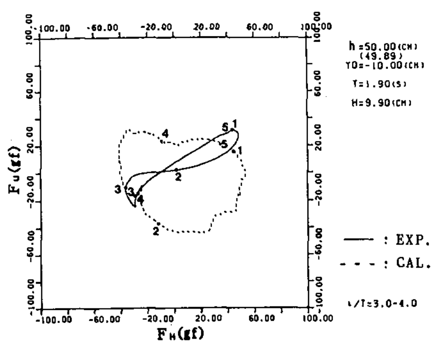

diagrams of Figures 7 (a) and (b) were obtained under the condition of $T_c$ = T, and those in the lower diagrams were under the condition of $T_c$ = T/2.

Looking at these diagrams, we can observe the following facts : 1) in the deeper water wave condition, the wave force path (C type) was simulated well under either conditions of $T_c$ = T or $T_c$ = T/2, and 2) however in the shallower water wave condition, the 8-shaped type wave force path (E type) was reproduced well under the condition of $T_c$ = T/2, but not under the condition of $T_c$ = T. In order to make clear the reason why such a difference as stated in 2) happened, the calculated flow induced by the vortices in the vicinity of a circular cylinder for Case W-3 were displayed. From these diagrams, we could observe that the unsymmetrical vortex behavior was reproduced at the time step of t/T = 3.6~3.8 for $T_c$ = T/2, but not for $T_c$ = T. Therefore we can conclude that appropriate decay of vortex should be introduced to simulate the interested flow characteristics.

(3) Drag coefficient, inertia coefficient, and lift coefficient

By using the calculated time histories of horizontal wave force component in a uniformly oscillating flow, the dag coefficient, $C_D$, and the inertia coefficient, $C_M$, were calculated through the following equations

$$C_D = \frac{3}{8}\int_0^{2\pi} \frac{F \sin\theta}{\rho R \hat{U}^2 \ell}\, d\theta \tag{14}$$

$$C_M = \frac{\hat{U}\, T}{2\pi^3 R} \int_0^{2\pi} \frac{F \cos\theta}{\rho R \hat{U}^2 \ell}\, d\theta \tag{15}$$

The obtained data for the symmetrical flow cases were plotted and compared with the laboratory data of Sarpkaya (1975) as shown in Figure 8. The abscissa in these diagrams is the K.C. number. The agreement for $C_M$ is fairly good, however the calculated values of $C_D$ were underestimated. The main reason why the latter discrepancy appeared is in the condition applied for determing the separation point. In this treatment the potential flow velocity surrounding the circular cylinder with the effect of vorticies was used. That is to say, at the point where the velocity is zero flow separation does not occur at any time and this fact caused rapid migration of separation point. Due to the above circumstance the development of vortex is disturbed, hence the drag coefficient results in decrease.

On the other hand two kinds of lift coefficient were calculated by using the following equations,

$$C_{L(MAX)} = \hat{F}_L / \rho \hat{U}^2 R \ell \tag{16}$$

$$C_{L(RMS)} = \sqrt{\overline{F_L^2}} / \rho \hat{U}^2 R \ell \tag{17}$$

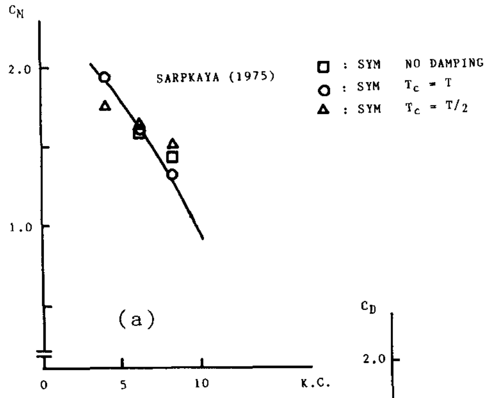


Fig.8

Comparison between calculated ones and laboratory curve for $C_M$ and $C_D$.

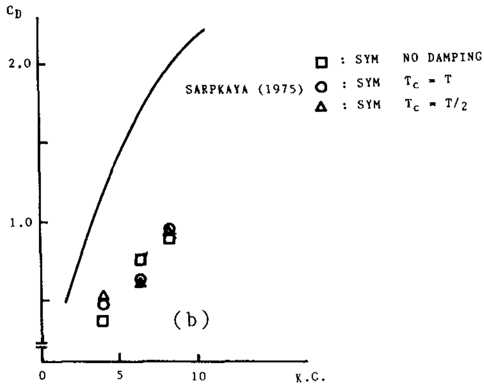


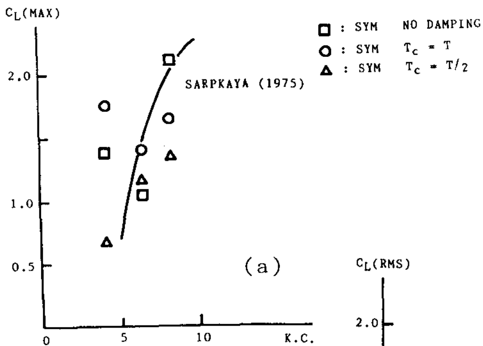


Fig.9

Comparison between calculated ones and laboratory curves for $C_L$.

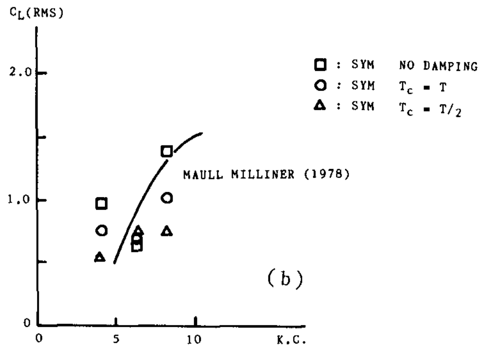

The former and latter data for symmetrical flow cases were compared with the laboratory data of Sarpkaya (1975), and that of Maull and Milliner (1978) as shown in Figures 9 (a) and (b) respectively. The abscissa of the diagrams is again the K.C. number. The tendency of scattered data agrees with the laboratory curve in both cases.

In the same way, these three coefficients for unsymmetrical flow cases were invertigated. The unsymmetry of flow did not induce any strong influence on the coefficients of $C_D$ and $C_M$, but induced a certain amount of influence on the coefficient of $C_L$

## 4. CONCLUSIONS

In the present paper was presented the numerical calculation method for predicting the wave forces acting on a horizontal circular cylinder set in a certain range of water depth. The simulation model is based on the discrete vortex method. The adaptability of the present calculation method was checked by comparing the calculated results with available laboratory data. As a conclusion of the present treatment, we found that the method presented here is applicable by introducing approprate decay of vortex circulation even to the cases where the emitted vortices induce strong unsymmetrical fluid motion.

Further study is needed to present a reasonable method to evaluate the vortex decay in the above treatment and to extend the capacity of the present simulation method for calculating the interested wave forces under more realistie or practical conditions.

## REFERENCES

Borgman, L.E. : Computation of the ocean-wave forces on inclined cylinders, Trans. Amer. Geophys. Union, Vol.39, pp.885-888, 1958.

Chaplin, J.R. : On the irrotational flow around a horizontal cylinder in waves, Jour. App. Mech., Trans. ASME, Vol.46, pp.689-694, 1981.

Dean, R.G. : Stream function representation of nonlinear ocean waves, Jour. Geophys. Res., Vol.70, pp.4561-4572, 1965.

Grass, A.J. and P.H. Kemp : Flow visualization studies of oscillatory flow past smooth and rough circular cylinder, Mechanics of Wave-Induced Forces on Cylinders, Pitman, pp.406-420, 1979.

Koderayama, W. and A. Tashiro : On the wave forces acting on a submerged horizontal circular cylinder, Jour. Japanese Society of Naval Architects, No.143, pp.134-144, 1978 (in Japanese).

Masuda, S., A. Watanabe, and K. Horikawa : Wave forces acting on and velocity field of a circular cylinder set horizontally in wave, 40th Annual Conv. of JSCE, pp.II 541- 542, 1985 (in Japanese).

Maull, D.J. and M.G. Milliner : Sinusoidal flow past a circular cylinder, Coastal Eng., Vol.2, pp.149-168, 1978.

Milne-Thomson, L.H. : Theoretical Hydrodynamics, 4th ed., McMilliam, New York, 1968.

Morison, J.R., M.P. O'Brien, J.W. Johnson, and S.A. Schaaf : The forces exerted by surface waves on piles, Petroleum Trans. AIME, Vol.189, pp.149-157, 1950.

Nath, J.H. and T. Yamanoto : Forces from fluid around objects, Proc. 14th Coastal Engrg. Conf., pp.1808-1827, 1974.

Ogilvie, T.F. : First- and second-order forces on a cylinder submerged under a free surface, J. Fluid Mech., Vol.16, pp.451-472, 1963.

Rosenhead, L. : Formation of vorticies from a surface of discontinuity, Proc. Roy. Soc., A, Vol.134, pp.170-192, 1931.

Sarpkaya, T. : An analytical study of separated flow about circular cylinders, J. Basic Engrg., Trans. of ASME, Vol.90, pp.511-518, 1968.

Sarpkaya, T. : Forces on cylinders and spheres in sinusoidally oscillating fluid, J. App. Mech., Trans. of ASME, Vol.42 No.1, pp.32-37, 1975.

Sawamoto, M., H. Oniwa, and J. Kashiwai. : A consideration on an expression of wave forces acting on a circular cylinder in an oscillatory flow, 34th Annual Conv. of JSCE, pp.II 579- 580, 1979 (in Japanese).

Sawamoto, M. and K. Kikuchi : Uplift forces acting on a circular cylinder in an oscillatory flow, Proc. 26th Japanese Coastal Engrg. Conf., JSCE, pp.429-433, 1979 (in Japanese).

Tsuzuki, S., A. Watanabe, and K. Horikawa : Wave forces acting on a horizontal circular cylinder, 39th Annual Conv. of JSCE, pp.II 303- 304, 1984 (in Japanese).

Uekita, M. and H. Yamazaki : A study on inertia forces acting on a horizontal circular cylinder, Proc. 27th Japanese Coastal Engrg. Conf., JSCE, pp.358-362, 1980 (in Japanese).